Eur. Phys. J. Special Topics **227**, 1029–1038 (2018)
© EDP Sciences, Springer-Verlag GmbH Germany, part of Springer Nature, 2018
https://doi.org/10.1140/epjst/e2018-800036-5

THE EUROPEAN PHYSICAL JOURNAL SPECIAL TOPICS

Regular Article

Dynamics of map-based neuronal network with modified spike-timing-dependent plasticity

A.V. Andreev[1], E.N. Pitsik[1], V.V. Makarov[1], A.N. Pisarchik[1,2], and A.E. Hramov[1,a]

[1] REC "Artificial Intelligence Systems and Neurotechnology", Yuri Gagarin State Technical University of Saratov, Politechnicheskaya Str. 77, Saratov 410054, Russia
[2] Center for Biomedical Technology, Technical University of Madrid, Campus Montegancedo, 28223 Pozuelo de Alarcon, Madrid, Spain

Received 31 March 2018 / Received in final form 21 June 2018
Published online 12 December 2018

Abstract. The effect of adaptive coupling is studied in a neural network of randomly-coupled Rulkov maps. As an adaptive mechanism, we propose a modified spike-timing-dependent plasticity (STDP) rule with implemented homeostatic property. The comparison of the results of classical and modified STDP shows that the implication of homeostatic property results in significant changes in the network dynamics. Moreover, the neural network with modified STPD demonstrates much more pronounced dynamical changes when internal noise and stimulus amplitudes are varied. The use of the modified rule also leads to decreasing coherence and characteristic correlation time in the system.

1 Introduction

Brain is one of the most comprehensive dynamical systems. Different approaches, including physiological, biochemical, mathematical and informatics, are applied for studying brain dynamics. The consideration of the brain neural system as a network of coupled dynamical units is an efficient mathematical way to simulate a complex behavior of a real neural system. Numerous studies are devoted to a study of structural properties of such neural networks, that can help in better understanding of dynamical properties of real synaptically connected neural networks [1].

There are two main reasons why the development of effective neural models is an important. First, a good mathematical model can give a deep insight into mechanisms responsible for memory, decision-making, and various forms of sensory information processing. Despite differences between fundamental factors underlying these processes in real neural networks and in models, they all can be explained by the neuroplasticity [2] observed on a microscopic level, as changes in the particular group of neurons, and on a macroscale level, as the interaction in cortical areas. Neuroplasticity reflects the neural network ability to change its structure according to its temporal dynamics. In neural models, this phenomenon is accounted by the

[a] e-mail: hramovae@gmail.com

formation of various forms of network connectivity structures under the influence of external stimuli.

Another reason of the importance of mathematical modeling is the development of effective artificial intelligent systems which use decision-making and control algorithms based on neuromorphic principles of information processing. The discovery of cognitive mechanisms underlying perception of various forms of stimuli allows a significant increase in the efficiency of the program methods employed in different neurobiological devices, such as neurofeedback-based neurointerfaces [3,4], exoskeletons [5], and prosthetic devices [6]. Besides the biomedical aspect, the technologies developed on the base of existing knowledge on brain functioning are actively used in machine learning methods [7].

In this paper, we introduce a adaptive neuronal network model based on the Rulkov map. The Rulkov model simulates a spiking-bursting behavior of a biological neuron. It is used for studying neural synchronization [8–10] which is an essential issue in neuroscience considering neural information processing and various pathological states, such as, for example, epileptic seizures. We study spatio-temporal patterns of neuronal behavior caused by the interplay of synchronization between neurons and structural adaptation in the network. We reveal the coherence resonance phenomenon in the Rulkov map network model, that occurs when the network undergoes stochastic perturbations which make the oscillatory network response more regular [11]. This effect manifests itself as an increase in the order (or coherence) of the dynamical system at the certain level of external and/or internal noise [12]. Such a behavior were observed in various dynamical systems and intensively studied in neural networks recently [11]. Here, we focus on the intrinsic noise effect on the network coherence and evaluate the optimal level of noise intensity, when the regularity in the neuron dynamics optimizes.

The network topology is regulated by spike-timing-dependent plasticity (STDP) based on the adaptation mechanism, which represents the Hebbian learning rule, the biologically inspired mechanism explaining temporal requirements for neural connectivity [13]. STDP characterizes how the temporal order of presynaptic and postsynaptic neural activity affects firing patterns in the network structure implemented by such forms of synaptic plasticity as long-term potentiation (LTP) and long-term depression (LTD) [14]. STDP is observed in different brain areas of insects and mammals [15–17]. It should be noted that classic STDP regulates the behaviour of two coupled neurons and does not reflects homeostasis phenomenon, which is an important feature that causes the emergence of non-homogeneous topologies in real-world neural networks.

In recent papers [18,19], the scientists studied synchronization phenomena in spiking neural networks with classical spike-timing-dependent plasticity, and showed that spiking synchronization can be improved by using STDP. In our work, we study dynamical regimes of neuronal networks taking into account the homeostasis term and consider the effect of intrinsic noise on the network coherence. We show that implementing the modified STDP rule significantly changes the system dynamics as compared with the classical STDP rule. As a result, the modified rule allows completely different dynamical regimes for the same parameters, because the system becomes more sensitive to external perturbations, such as a constant stimulus or noise. Since the influence of the external signal is more significant, less experimental resources are required to control the system dynamics.

2 Model

The ensemble of coupled Rulkov maps can be described by a set of equations, where each i-th neuron is represented as [20]

$$\begin{aligned} x_{n+1} &= f(x_n, x_{n-1}, y_n + \beta_n), \\ y_{n+1} &= y_n - \mu(x_n + 1) + \mu\sigma + \mu\sigma_n + \mu A^{\xi}\xi_n. \end{aligned} \tag{1}$$

Here, x is the fast dynamical variable that represents the membrane potential of the i-th neuron and y is the slow gating variable dependent on the small value of $\mu \in (0, 1]$. Parameters α, σ, μ stand for network dynamic regulation, and A^{ξ} is the amplitude of Gaussian noise ξ, which has zero mean and unity standard deviation. Function f describes different types of neuron-like activity corresponding to spiking, bursting and silent regimes as

$$f(x_n, x_{n-1}, y_n) = \begin{cases} \alpha/(1 - x_n) + y_n, & \text{if } x_n \leq 0, \\ \alpha + y_n, & \text{if } 0 < x_n < \alpha + y_n \text{ and } x_{n-1} \leq 0, \\ -1, & \text{if } x_n \geq \alpha + y_n \text{ or } x_{n-1} > 0. \end{cases} \tag{2}$$

The external stimulation is introduced via variables β_n and σ_n defined as

$$\begin{aligned} \beta_n &= \beta^e I_n^{ext} + \beta^{syn} I_n^{syn}, \\ \sigma_n &= \sigma^e I_n^{ext} + \sigma^{syn} I_n^{syn}, \end{aligned} \tag{3}$$

where β^e and σ^e are the coefficients used to balance the effect of external current I_n^{ext}:

$$I_n^{exp} = \begin{cases} 0, & n < t_s, \\ A, & n \geq t_s, \end{cases} \tag{4}$$

where A is the amplitude of external stimulus, β^{syn} and σ^{syn} are the coefficients of chemical synaptic coupling [21], and I_n^{syn} is the synaptic current given as

$$I_{n+1}^{syn} = \gamma I_n^{syn} - g_{syn} * \begin{cases} (x_n^{post} - x_{rp})/(1 + e^{-k(x_n^{post} - \theta)}), & x_n^{pre} \geq \alpha + y_n^{pre} + \beta_n^{pre}, \\ 0, & x_n^{pre} < \alpha + y_n^{pre} + \beta_n^{pre}, \end{cases} \tag{5}$$

where $g_{syn} \geq 0$ is the strength of synaptic coupling, $\theta = -1.55$ and $k = 50$ are the synaptic parameters which stand for the synaptic threshold behavior. The superindices *pre* and *post* refer to the presynaptic and postsynaptic variables, respectively, $\gamma \in [0, 1]$ is the synaptic relaxation time defining a synaptic current portion preserved in the next iteration, and x_{rp} is the reversal potential determining the synapse type, inhibitory or excitatory. We consider a motif of $N = 100$ globally coupled neurons with coupling strength g_{syn} uniformly distributed in the interval of $[0.0, 0.1]$ and relaxation time γ uniformly distributed in $[0.0, 0.5]$. The parameter values are chosen so that the uncoupled neurons are in a resting state, namely, $\alpha = 3.65$, $\sigma = 0.06$, and $\mu = 0.0005$. We also assume the following parameter values: $\beta^e = 0.133$, $\sigma^e = 1.0$, $\beta^{syn} = 0.1$, $\sigma^{syn} = 0.5$, and $x_{rp} = 0$. Applying the external stimulus to the system for these parameter values forces the neurons from a silent to a spiking regime. The values of α and σ allow us to switch the neurons to a bursting regime.

To evaluate correlation in our model, we introduce the characteristic correlation time [12]:

$$\tau_c = \sum_{t_0}^{T} C(\tau)^2, \tag{6}$$

where $t_0 = 3000$ is the number of iterations in transients, T is the total number of iterations in time series, and $C(\tau)$ is the autocorrelation function given as

$$C(\tau) = \frac{\left\langle \left(x_{avr}(n) - \langle x_{avr}\rangle\right)\left(x_{avr}(n+\tau) - \langle x_{arv}\rangle\right)\right\rangle}{\left\langle \left(x_{avr}(n) - \langle x_{avr}\rangle\right)^2\right\rangle}, \tag{7}$$

where $\langle ... \rangle$ is the time average after transients and x_{avr} represents the averaged membrane potential. The small value of the correlation time indicates an uncorrelated system behaviour. Thus, the larger the τ_c, the better the regularity (coherence).

To evaluate synchronization in the neuronal network, we introduce synchronization degree [22,23]:

$$S = \sqrt{\frac{1}{T - t_0}\int_{t=t_0}^{T} s(t)dt}, \tag{8}$$

where $s(t)$ is defined as

$$s(t) = \frac{1}{N}\sum_{n=1}^{N}[x_n(t)]^2 - \left[\frac{1}{N}\sum_{n=1}^{N} x_n(t)\right]^2, \tag{9}$$

and N stands for the number of nodes ($n = 1, 2, ..., N$). The smaller S, the more network elements are in a synchronous state, $S = 0$ means complete synchronization in the neuronal network.

Coherence is defined as

$$H = \frac{1}{N}\sum_{n=1}^{N} h_n^2 - \left(\frac{1}{N}\sum_{n=1}^{N} h_n\right)^2, \tag{10}$$

and h_n is described by the equation:

$$h_n = \sqrt{\frac{1}{M - t_0 + 1}\sum_{m=m_0}^{M} R_m(n)}, \tag{11}$$

where R_m is interspike interval (ISI) between m-th and $(m+1)$-th spike, M is the number of spikes ($m = 1, 2, ..., M$), m_0 is the number of transient spikes. The second condition in equation (2), which defines the spike generation threshold, is used to determine ISIs.

The standard STDP learning rule is defined by equation:

$$\triangle g_{ij} = A^+(g_{ij})x_j\delta^i - A^-(g_{ij})x_i\delta^j, \tag{12}$$

where δ is the delta function, A^+ and A^- denotes how much the coupling strength will be changed from pre- and postsynaptic spike generation, respectively. In this

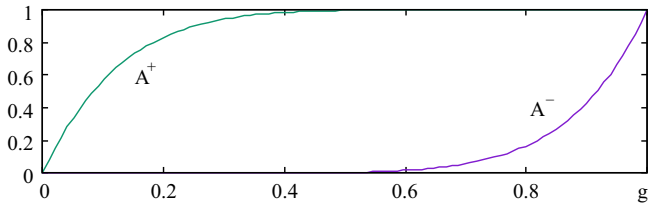

Fig. 1. The dependencies of STDP parameters A^+ and A^- on the synaptic weight.

work, we apply these values as a function of the current value of the synaptic weight g_{ij} as follows

$$A^+(g) = 1 - g^8, \qquad A^-(g) = g^8. \tag{13}$$

This allows us to bound the coupling strength in the range [0, 1], as shown in Figure 1.

Although this classical mechanism for synaptic plasticity regulates the interaction between pre- and post-synaptic neuron, it does not take into account the homeostatic plasticity whose presence is essential in real neural networks [26]. It was recently shown that in adaptive networks, the implementation of this property can cause the emergence of non-homogeneous real-like topologies [27]. In the present research, we implement the homeostatic property by adding the term which describes the interaction of the current node with all other connected neurons [28]:

$$\Delta g_{ij} = A^+(g_{ij})x_j\delta^i - A^-(g_{ij})x_i\delta^j + \sum_{k\neq j}(A^+(g_{ik})x_k\delta^i - A^-(g_{ik})x_k\delta^k), \tag{14}$$

where the first and second terms in the right part of the equation correspond to the interaction between nodes i and j, and the third term corresponds to the average impact of all other nodes connected to node i [29]. Such a notation allows the account of a synaptic scaling process (or homeostatic scaling), in which the neural network regulates chronically elevated activity [30].

3 Results

To estimate the system dynamics in the response to control parameters α and σ, we study synchronization degree in the two-parameter space of the coherence and correlation time calculated for both classic equation (12) and modified equation (14) STDP models, shown in Figure 2. The black areas in Figures 2a and 2b correspond to complete synchronization when $S = 0$, while the white areas in Figures 2e and 2f indicate a silent regime characterized by the absence of spiking activity. An increase in α with constant σ leads to enhancing coherence and synchronization. If we fix α and increase σ, we observe an increase in both S and H. The comparison of the results based on classical STDP principles (Figs. 2a and 2e) and on our approach (Figs. 2b and 2d) allows us to conclude that the change in the STDP rule does affect the (α, σ)-parameter dependencies of coherence and synchronization degree.

In Figures 2e and 2f one can distinguish three typical areas (white, yellow/red, and blue/black) corresponding to high, medium, and low values of τ_c, respectively. Comparing these figures with the bifurcation diagram on the (α, σ)-parameter plane in reference [25], where three different regimes (silence, bursts of spikes, and spikes)

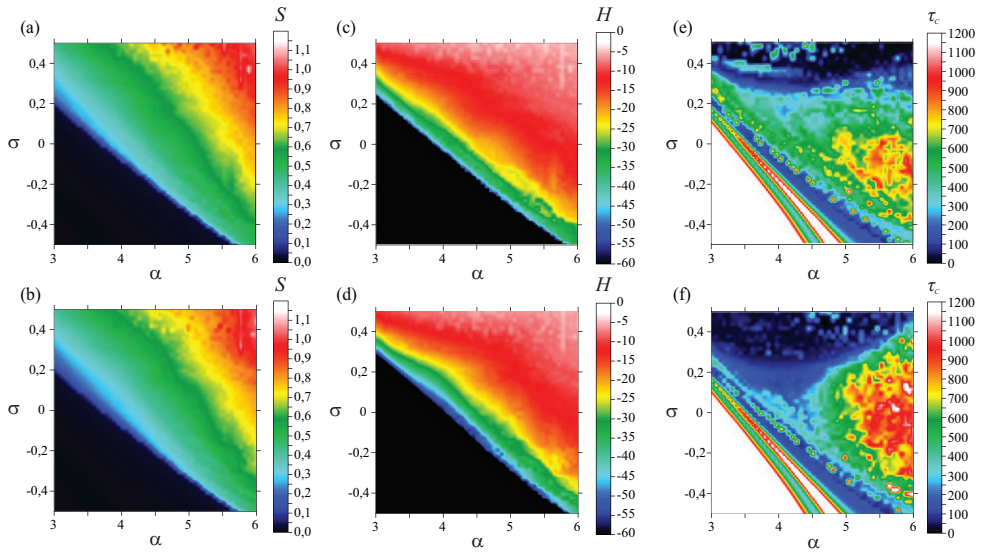

Fig. 2. Network characteristics in the (α, σ)-parameter space, calculated using classical STDP principles (a,c,e) and on the base of our approach (b,d,f) for $A = 1$, $A^{\xi} = 0.5$. (a,b) Synchronization degree S, (c,d) coherence H, and (e,f) correlation time τ_c.

are depicted, one can see a very close similarity. To verify this result, we calculate time series of averaging membrane potentials as follows [11]

$$x_{avr} = \frac{1}{N} \sum_{i=1}^{N} x_i, \tag{15}$$

where i is the neuron index and $N = 150$ is the total number of neurons in the network. In Figures 3a and 3c, these averaging signals occur in the blue/black and yellow/red areas which correspond to the regimes of spikes and bursts of spikes, respectively. One can see that a change in the STDP rule leads to corresponding change in the characteristic correlation time map. The main difference between Figures 2e and 2f lies in the area of $\alpha \in [3; 4.6]$, $\sigma \in [0; 0.3]$. In the time series of averaging membrane potentials from this area (Fig. 3b), the network with classic STDP principles demonstrates bursting dynamics, while the network with STDP rule proposed in this study exhibits spiking dynamics.

The comparison of Figures 2e and 2f with the bifurcation diagram from reference [25] demonstrates that a change in the STDP rule in the way we do in this paper allows us to save the map of characteristic regimes of a single neuron. At the same time, the use of the classic STDP principles change the regime map and increae the area of bursts of spikes.

To estimate the network response to noise and external stimuli, we study two-parameter dependencies of synchronization degree, coherence, and correlation time on noise (A^{ξ}) and external stimulus (A) amplitudes, calculated for both classic (Eq. (12)) and modified (Eq. (14)) STDP models, as shown in Figure 4. One can see that synchronization degree increase a bit faster when the first learning design is applied (Fig. 4a); in the classical model, the value of $A > 1.5$ is enough to obtain $S \geq 0.7$, while the modified model requires larger amplitude values. This can be a direct consequence of the presence of the third term in equation (14). When the STDP learning takes into account the dynamics of all synaptic connections of the current

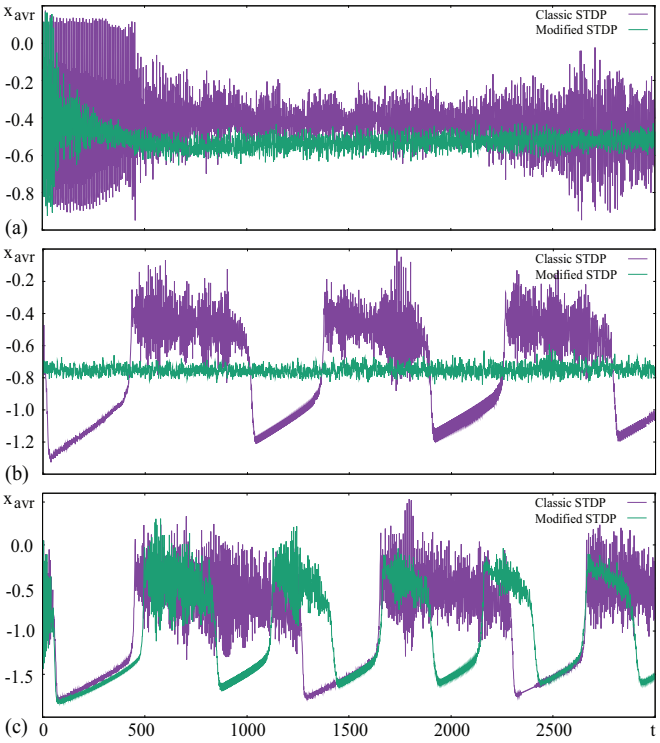

Fig. 3. Time series of average membrane potential for classical STDP principles (green) and proposed in this study (blue) for $A = 1$, $A^{\xi} = 0.5$ and (a) $\alpha = 3.5$, $\sigma = 0.45$, (b) $\alpha = 3.75$, $\sigma = 0.2$, and (c) $\alpha = 5.5$, $\sigma = 0.0$.

element with all other elements, the dynamics of whole network evolves differently, in presumably more realistic way. Besides, we do not observe the influence of A^{ξ} on the network dynamics, although some combinations of A^{ξ} and A values (e.g., $A^{\xi} \approx 0.6$, $A \approx 1.6$, where there is a red spot on Fig. 4b) result in the high S value.

One can note correlations between dependencies shown in Figures 4c–4f. Considering coherence dynamics shown in Figures 4c and 4d, one can distinguish similar patterns corresponding to the classic and modified STDP models. In the classical model (Fig. 4c), the system reaches minimal coherence with a large value of the noise amplitude ($A^{\xi} > 1.8$) and a small value of the external stimulus ($A < 0.3$). In the contrary, the maximal coherence corresponds to intensive external stimuli and faint noise ($A^{\xi} < 0.5$ and $A > 1.5$). A similar situation occurs with the modified system (Fig. 4d), although the coherence value overcomes notable depression.

Finally, Figures 4e and 4f illustrate correlations between noise and external stimuli amplitudes and correlation time, which also demonstrate a high coherence level in the system. Indeed, one can track a set of similarities between dynamics of τ_c value in the classical and modified models in Figures 4e and 4f, respectively, as well as the correlations between H and τ_c in the corresponding models. In both cases, the value of correlation time decreases as the noise amplitude is increased, and reaches a maximum value for $A^{\xi} < 1$.

Despite the observed differences, we can conclude that, generally, the dynamical patterns remain the same in both models. The whole picture reveals the tendency of the considered characteristics to suppress in the case of the modified model, but the

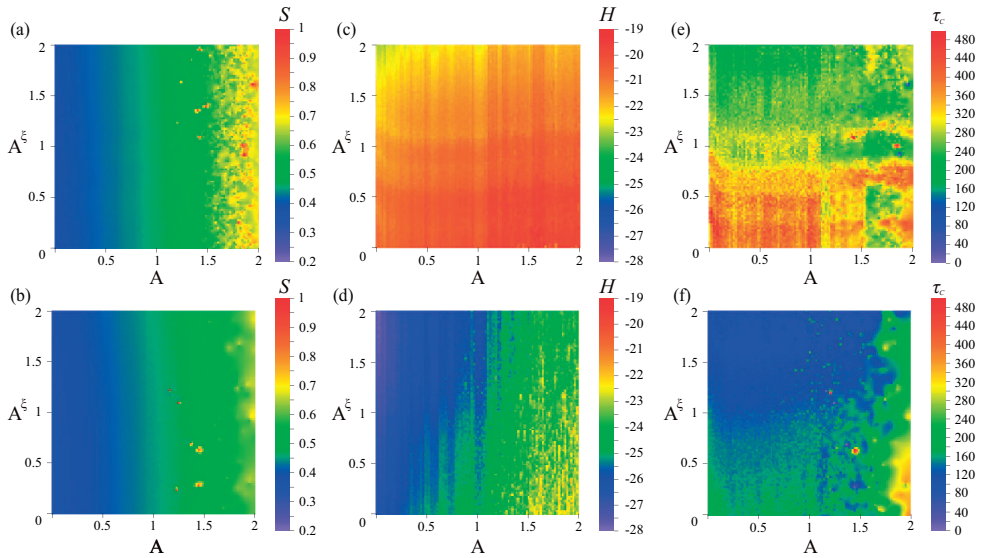

Fig. 4. Two-parameter dependencies of network characteristics on noise (A^{ξ}) and external stimulus (A) amplitudes, calculated for classic STDP principles (a,c,e) and proposed in this study (b,d,f). (a,b) Synchronization degree S, (c,d) coherence H, and (e,f) correlation time τ_c.

key correlations, such as growing coherence in the presence of noise with increasing amplitude and correlations between τ_c and H, appear equally.

4 Conclusion

We have studied the dynamics of the neuronal network of the Rulkov maps using the modified STDP-learning rule by implementing the homeostatic property [29]. This property was employed by the additional component in the STDP equation, which described the average connectivity change of the current node for the single time step. By this way, we took into account the impact of all neighbours of the node on the formation of each of its connections [28].

We have investigated the network of 150 Rulkov neurons coupled to each other with random weights, which were changed through time according to the classical and modified STDP principles in the presence of noise and external stimulus. We have found that the implication of homeostatic property in the STDP rule led to sufficient changes in the dynamics as compared with the classical mechanism. At this point, the whole network dynamics became similar to that of a single neuron; the number of the neurons in the burst-of-spike regime decreased.

Besides the neuron parameters, we have also investigated the influence of noise and external stimulus on the network dynamics. We have found that the system with the modified STPD demonstrated much more pronounced dynamical changes when noise and stimulus amplitudes were varied. Using the modified rule also led to decreasing coherence and characteristic correlation time in the system, that can be important for applications in computational models for pattern classification.

Recent research implies the possibility for implication of networks composed by spiking neurons for the solution of intellectual tasks, such as classification of brain states, that earlier could only be adressed to classical non-dynamical neural

networks. At the same time, the main requirement allowing to shape the dynamics and topology of spiking networks for a concrete task is the implementation of the biologically inspired adaptive mechanism, including the rewarded plasticity as in reference [31]. The results obtained in the present paper can be used for the development of biologically inspired intelligent systems for pattern recognition [32] of adaptive locomotion [33].

This work has been supported by the Russian Science Foundation (grant 17-72-30003).

Author contribution statement

A.V.A. and V.V.M. designed the model and computational framework, performed simulations, and analyzed the data. A.V.A., E.N.P. and V.V.M. wrote the manuscript draft. A.N.P. and A.E.H. conceived the study, planed and directed the research, and corrected the final version of the manuscript.

References

1. O.V. Maslennikov, V.I. Nekorkin, Phys. Usp. **60**, 694 (2017)
2. B. Draganski, C. Gaser, V. Busch, G. Schuierer, U. Bogdahn, A. May, Nature **427**, 311 (2004)
3. H.J. Hwang, K. Kwon, C.H. Im, J. Neurosci. Methods **179**, 150 (2009)
4. V.A. Maksimenko, S. Heukelum, V.V. Makarov, J. Kelderhuis, A. Luttjohann, A.A. Koronovskii, A.E. Hramov, G. van Luijtelaar, Sci. Rep. **7**, 2487 (2017)
5. A.M. Dollar, H. Herr, IEEE Trans. Robot. **24**, 144 (2008)
6. M. Haugland, T. Sinkjær, Technol. Health. Care **7**, 393 (1999)
7. N.M. Nasrabadi, J. Electron. Imaging **16**, 049901 (2007)
8. D. Hu, H. Cao, Commun. Nonlinear Sci. Numer. Simul. **35**, 105 (2016)
9. H. Sun, H. Cao, Commun. Nonlinear Sci. Numer. Simul. **40**, 15 (2016)
10. S. Boccaletti, A.N. Pisarchik, C.I. del Genio, A. Amann, *Synchronization: from coupled systems to complex networks* (Cambridge University Press, 2018)
11. A.V. Andreev, V.V. Makarov, A.E. Runnova, A.N. Pisarchik, A.E. Hramov, Chaos Solitons Fractals **106**, 80 (2018)
12. A.S. Pikovsky, J. Kurths, Phys. Rev. Lett. **78**, 775 (1997)
13. S. Song, K.D. Miller, L.F. Abbott, Nat. Neurosci. **3**, 919 (2000)
14. C. Clopath, L. Busing, E. Vasilaki, W. Gerstner, Nat. Neurosci. **13**, 344 (2010)
15. D.E. Shulz, D.E. Feldman, in *Neural circuit development and function in the brain* (Academic Press, 2013), p. 155
16. E.M. Izhikevich, G.M. Edelman, Proc. Natl. Acad. Sci. U.S.A. **105**, 3593 (2008)
17. P. Arena, S. De Fiore, L. Patanè, M. Pollino, C. Ventura, in *Proceedings of the 2010 International Joint Conference on Neural Networks* (2010) pp. 1–8
18. N. Shibuya, C. Unsworth, Y. Uwate, Y. Nishio, in *IEEE Workshop on Nonlinear Circuit Networks* (2013), pp. 61–64
19. R.R. Borges, F.S. Borges, E.L. Lameua, A.M. Batistaa, K.C. Iarosz, I.L. Caldas, R.L. Viana, M.A.F. Sanjuán, Commun. Nonlinear Sci. Numer. Simul. **34**, 12 (2016)
20. N.F. Rulkov, I. Timofeev, M. Bazhenov, J. Comput. Neurosci. **17**, 203 (2004)
21. D. Hu, H. Cao, Commun. Nonlinear Sci. Numer. Simulat. **35**, 105 (2016)
22. Q. Wang, M. Perc, Z. Duan, G. Chen, Phys. Rev. E **80**, 026206 (2009)
23. J.M. Sausedo-Solorio, A.N. Pisarchik, Eur. Phys. J. Special Topics **226**, 1911 (2017)
24. J.S. Bendat, A.G. Piersol, *Random data: analysis and measurement procedures* (John Wiley and Sons, New York, Sydney, London, 2011)
25. A.L. Shilnikov, N.F. Rulkov, Int. J. Bifurc. Chaos **13**, 3325 (2003)

26. W. Wallace, M.F. Bear, J. Neurosci. **24**, 6928 (2004)
27. V.V. Makarov, A.A. Koronovskii, V.A. Maksimenko, A.E. Hramov, O.I. Moskalenko, J.M. Buldú, S. Boccaletti, Chaos Solitons Fractals **84**, 23 (2016)
28. R. Gutierrez, A. Amann, S. Assenza, J. Gomez-Gardenes, V. Latora, S. Boccaletti, Phys. Rev. Lett. **107**, 234103 (2011)
29. A.J. Watt, N.S. Desai, Front. Synaptic Neurosci. **2**, 5 (2010)
30. E. Marder, J.M. Goaillard, Nature Rev. Neurosci. **7**, 563 (2006)
31. S. Skorheim, P. Lonjers, M. Bazhenov, PLoS One **9**, e90821 (2014)
32. N. Kasabov, K. Dhoble, N. Nuntalid, G. Indiveri, Neural Netw. **41**, 188 (2013)
33. G. Indiveri, E. Chicca, R. Douglas, IEEE Trans. Neural Netw. **17**, 211 (2006)